SCALE-BY-SCALE NON-EQUILIBRIUM DRIVEN BY NON-HOMOGENEITY IN THE CENTRAL REGION OF TURBULENT CHANNEL FLOW

Jiamei LI
Univ. Lille, CNRS, ONERA, Arts et Metiers Institute of Technology,
Centrale Lille Institut, UMR 9014 - LMFL, F-59000 Lille, France
jiamei.li@centralelille.fr

Christos VASSILICOS
Univ. Lille, CNRS, ONERA, Arts et Metiers Institute of Technology,
Centrale Lille Institut, UMR 9014 - LMFL, F-59000 Lille, France
john-christos.vassilicos@cnrs.fr

ABSTRACT

Compared with the near-wall and near-equilibrium regions of fully developed turbulent channel flow (FD TCF) where non-homogeneity is introduced by both mean shear and non-linear turbulent diffusion in the near-wall region and only mean shear/turbulence production in the near-equilibrium region, the core region is only affected by non-linear turbulent diffusion and is locally non-homogeneous down to scales smaller than the Taylor length scale. This non-homogeneity gives rise to a scale-by-scale cascade that is out of Kolmogorov equilibrium where the inter-space turbulent energy transfer rate is comparable to the inter-scale turbulent energy transfer rate at all scales. Both are negative and equal to a constant fraction of average turbulent dissipation rate with a logarithmic correction over an inertial range of two-point separations in both homogeneous directions. They sum up to minus the turbulence dissipation rate plus a small or vanishing pressure-related transfer rate contribution.

INTRODUCTION

Qualitatively, the turbulence cascade is a central universal aspect of turbulence in all fully developed turbulent flows. No decisive advance in turbulence theory and modelling can be imagined without significant progress in our understanding of turbulence cascades as they determine inter-scale turbulent energy transfer rates. For stationary homogeneous turbulence, Kolmogorov showed in 1941 that the average inter-scale transfer rate is in equilibrium with the average turbulence dissipation rate over the inertial range of scales at high Reynolds numbers (Frisch, 1995). However, this scale-by-scale equilibrium is not applicable to non-stationary and/or non-homogeneous turbulence. Chen & Vassilicos (2022) and Beaumard *et al.* (2024) developed a theory for non-homogeneous turbulence and predicted a constant inter-scale and inter-space turbulence transfer rates over the inertial range for turbulent flows without turbulence production from mean shear. Experiment support for this prediction was obtained under the rotating impeller of a turbulent mixer (Beaumard *et al.*, 2024) and on the centreline of turbulent plane wakes of nearby pairs of square prisms (Noriega & Vassilicos, 2026). Here we consider direct numerical simulations (DNS) of FD TCF which are non-homogeneous in the direction normal to the upper and lower walls and periodic in the two wall-parallel directions. In the near-equilibrium region of this turbulent flow, Apostolidis *et al.* (2023) showed that turbulence production is important over all inertial scales and that the scale-by-scale inter-scale transfers are therefore out of Kolmogorov equilibrium over length scales as small as the Taylor length λ. Here we study inter-scale turbulent energy transfers in the FD TCF's centreline region where turbulence production is negligible but inter-space transport becomes of importance.

TWO-POINT TURBULENT ENERGY EQUATION

Our study is based on the scale-by-scale two-point turbulent energy budget equation obtained directly from the Navier-Stokes equations and the Reynolds decomposition by Hill (2002):

$$
\begin{aligned}
\underbrace{\langle \frac{\partial}{\partial t}\delta u_i^2\rangle}_{D_t} = & -\underbrace{\langle \frac{\partial}{\partial r_k}\delta U_k \delta u_i^2\rangle}_{\Pi_U} - \underbrace{\langle \frac{\partial}{\partial x_k} u_k^* \delta u_i^2\rangle}_{T_u} - \underbrace{\langle \frac{\partial}{\partial r_k}\delta u_k \delta u_i^2\rangle}_{\Pi} \\
& \underbrace{-2\langle \delta u_i \frac{\partial}{\partial x_i}\delta p\rangle}_{T_p} \underbrace{-2\langle v^* \delta u \frac{d}{dy}\delta U\rangle - 2\langle \delta v \delta u \frac{d}{dr_y}\delta U\rangle}_{P} \\
& + \underbrace{\frac{\nu}{2}\langle \frac{\partial^2}{\partial x_k^2}\delta u_i^2\rangle}_{D_x} + \underbrace{\frac{\nu}{2}\langle \frac{\partial^2}{\partial r_k^2}\delta u_i^2\rangle}_{D_r} - \underbrace{\nu\langle (\frac{\partial}{\partial x_k}\delta u_i)^2 + (\frac{\partial}{\partial r_k}\delta u_i)^2\rangle}_{\varepsilon}
\end{aligned}
\tag{1}
$$

with implicit summations over $i = 1,2,3$ and $k = 1,2,3$. The Reynolds decomposition of the fluid velocity component $\hat{u}_i$ is $\hat{u}_i = U_i + u_i$ with $U_i = \langle \hat{u}_i \rangle$ where the brackets signify averaging over time and homogeneous (streamwise and spanwise) directions. Similarly, the pressure per unit mass density is $\hat{p} = P + p$ with $P = \langle \hat{p} \rangle$, and two-point fluctuation differences are $\delta u_i = \frac{1}{2}(u_i(\mathbf{x}+\mathbf{r},t) - u_i(\mathbf{x}-\mathbf{r},t))$ whereas two-point fluctuation sums are $u_i^* = \frac{1}{2}(u_i(\mathbf{x}+\mathbf{r},t) + u_i(\mathbf{x}-\mathbf{r},t))$. The coordinates of the centroid $\mathbf{x}$ and the two-point separation vector

Table 1. Summary of DNS datasets of FD TCF.

Re_τ	L_x/δ	L_z/δ	N_x	N_y	N_z	N_f
934	8π	3π	2048	385	1535	10
3000	6π	1.5π	5120	768	2048	8

$\mathbf{r}$ are, respectively, x, r_x in the streamwise, y , r_y in the wall-normal and z , r_z in the spanwise directions

By virtue of FD TCF statistical stationarity, $D_t = 0$ by FD TCF stationarity. If we limit ourselves to $\mathbf{r} = (r_x, 0, r_z)$, i.e. $r_y = 0$, then $\Pi_U = 0$ because $\delta U = 0$ for $r_y = 0$. In the centreline region the turbulence production P is negligible as a consequence of vanishing mean shear, and in the outer region the viscous diffusion term D_x is also negligible. Therefore, at wall distances y close to channel half width δ, eq(1) simplifies as follows for $\mathbf{r} = (r_x, 0, r_z)$:

$$0 = -T_u - \Pi + T_p + D_r - \varepsilon \tag{2}$$

where T_u is the non-linear inter-space transfer rate, Π is the non-linear inter-scale transfer rate, T_p is the rate of transfer by pressure-velocity correlations, ε is the average turbulence dissipation rate and D_r is the viscous diffusion rate in scale space which is small compared to ε, and therefore negligible, at scales larger than the Taylor length $\lambda = \sqrt{10\nu\langle K\rangle/\langle\varepsilon\rangle}$ (Valente & Vassilicos, 2015) where K is the local turbulent kinetic energy. (For a relation between the Taylor length and the average distance between stagnation points (to measure two-point separation distances with) as a function of wall-normal distance, see Dallas *et al.* (2009).)

A recent theory (Chen & Vassilicos, 2022; Beaumard *et al.*, 2024) based on an hypothesis of homogeneous two-point physics in non-homogeneous turbulence and an intermediate asymptotic analysis of equation (1) predicts the existence of an inertial range where all three non-linear transfer rates in equation (1) are, to leading order, constants independent of two-point separation in an inertial range of scales. This prediction has been made for the type of non-homogeneity dominated by turbulent transport/diffusion such that turbulence production and mean linear advection are negligible. Experimental support for this prediction has been obtained by (Beaumard *et al.*, 2024; Noriega & Vassilicos, 2026) in turbulent wakes and under the impeller inside a mixer. A related yet different prediction was made in the near-equilibrium layer of FD TCF (Apostolidis *et al.*, 2023) where the non-homogeneity is of a different nature: presence of turbulence production throughout the inertial range and absence of average turbulent transport. At the central region of a FD TCF, turbulent production and mean linear advection are also minor but the fluctuating pressure effects can be quite different from those in turbulent wakes or under a mixing impeller. Therefore, it is worth studying the scale-by-scale behaviour of the non-linear terms in equation (2) around the centreline of a FD TCF.

DNS DATASETS

The terms in equation (2) are evaluated from datasets obtained from direct numerical simulations (DNS) of FD TCF at $Re_\tau = 934$ (TCF934) by Hoyas & Jiménez (2008) and $Re_\tau = 3000$ (TCF3000) by Thais *et al.* (2011). The fields are well resolved and also large enough ($[8\pi\delta, 2\delta, 3\pi\delta]$ for TCF934 and $[6\pi\delta, 2\delta, 1.5\pi\delta]$ for TCF3000). For statistical convergence, more than 10 times δ/u_τ are available for TCF934 and more than 10 time δ/U_b (where U_b is the bulk velocity) are available for TCF3000. The summary of DNS datasets is shown in table 1 with the resolution in all three directions (N_x, N_y, N_z) and number of files (N_f) used for computing one-point and two-point statistics.

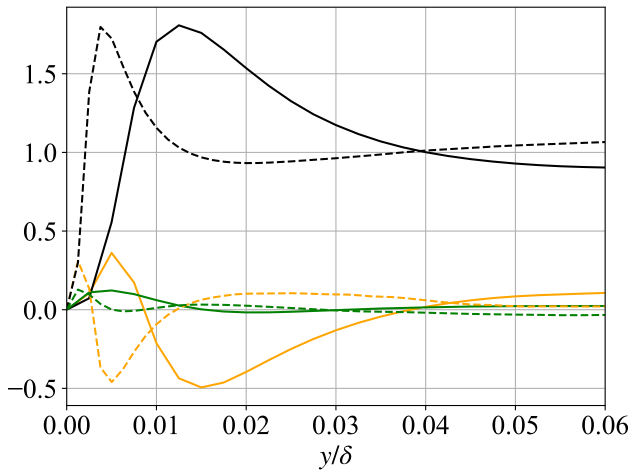

Figure 1. Profiles of dominant terms in the one-point turbulent kinetic energy budget for TCF934 (solid lines) and TCF3000 (dashed lines). The profiles are plotted versus y/δ in the near-wall region, with black lines for turbulent production rate, orange lines for turbulent transport rate and green lines for pressure transport rate. All terms are normalised by the average turbulent energy dissipation rate.

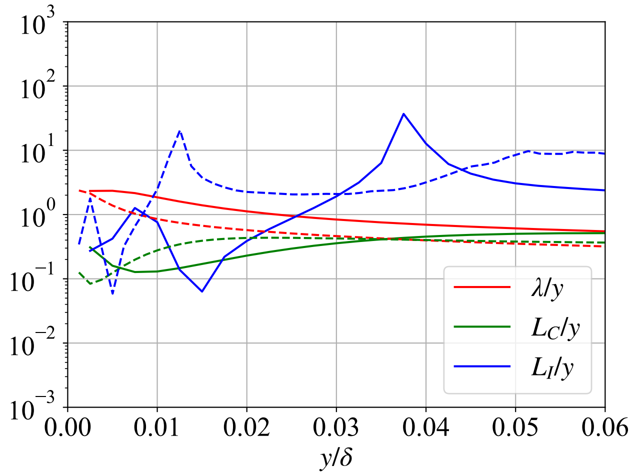

Figure 2. Profiles of the Taylor length λ, the Corrsin length scale L_C and non-homogeneity length scale L_I (reflecting non-linear turbulent transport). The profiles are plotted versus y/δ for TCF934 (solid lines) and TCF3000 (dashed lines) in the near-wall region. All scales are normalised by the distance from the wall y.

RESULTS

Non-homogeneity length scales

Statistical non-homogeneity can be characterised by non-homogeneity length-scales. In the case where the non-homogeneity is dominated by mean shear and turbulent pro-

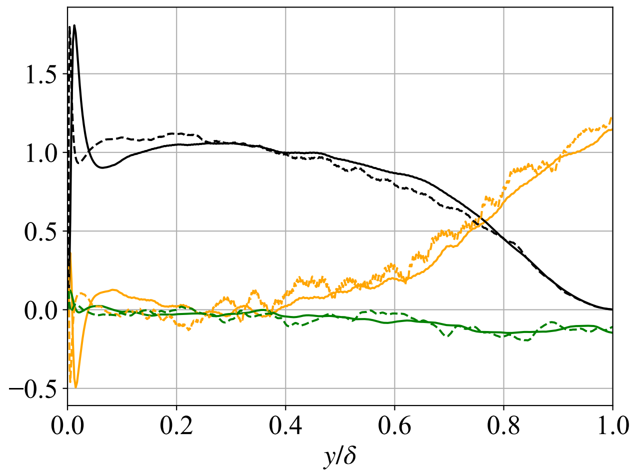

Figure 3. Profiles of dominant terms in the one-point turbulent kinetic energy budget of TCF934 (solid lines) and TCF3000 (dashed lines). The profiles are plotted versus y/δ, with black lines for energy production, orange lines for turbulent transport and green lines for pressure transport rate. All terms are normalised by the average turbulent energy dissipation rate.

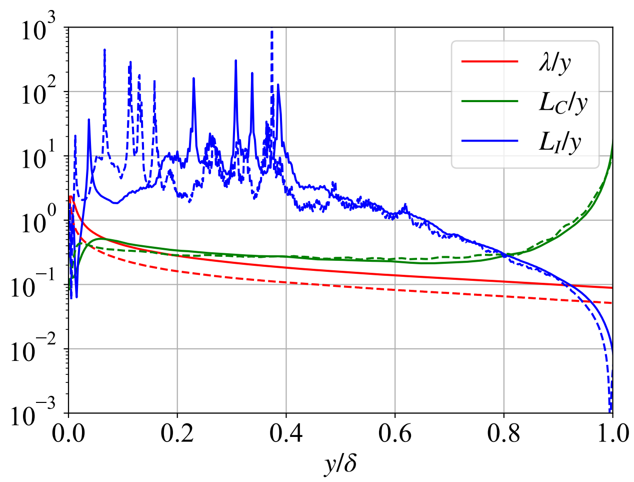

Figure 4. Profiles of the Taylor length λ, the Corrsin length scale L_C and non-homogeneity length scale L_I (reflecting non-linear turbulent transport). The profiles are plotted versus y/δ for TCF934 (solid lines) and TCF3000 (dashed lines). All scales are normalised by the distance from the wall y.

duction, the relevant length-scale is the Corrsin length-scale Corrsin (1958):

$$L_C = \sqrt{\frac{\langle \varepsilon \rangle}{S^3}} \tag{3}$$

where S is the mean shear rate. Scales larger than L_C are particularly sensitive to mean shear. (This is not the place to make a statement concerning scales smaller than L_C, one can consult see (Chen & Vassilicos, 2022; Apostolidis *et al.*, 2023) if interested.) If the non-homogeneity is dominated by significant non-linear turbulent transport without turbulence production, an appropriate non-homogeneity length-scale recently introduced by Noriega & Vassilicos (2026) is the ratio of the average turbulent energy flux to the gradient of this flux. In the context of FD TCF we define it as follows

$$L_I = \frac{|\langle u_2 K \rangle|}{|\langle \frac{\partial}{\partial y}(u_2 K) \rangle|} \tag{4}$$

where u_2 is the wall-normal fluctuating velocity. At scales larger than L_I the turbulent diffusion's non-homogeneity of the turbulence cannot be overlooked.

The length-scales λ , L_C and L_I are based on one-point statistics relating to the one-point turbulent kinetic energy budget. We therefore plot wall-normal profiles of dominant terms in this budget in figures 1 and 3. These figures give us some appreciation of the non-homogeneity of these terms. Figure 1 shows near-wall wall-normal profiles for $0 \le y/\delta \le 0.06$ and figure 2 shows wall-normal profiles of λ/y , L_C/y and L_I/y in the same y-range. Figure 3 shows wall-normal profiles from wall to centreline, i.e. $0 \le y/\delta \le 1$, and figure 4 shows wall-normal profiles of λ/y , L_C/y and L_I/y in the same y-range. In the near wall region ($y^+ \le 60$ where $y^+ = u_\tau y/\nu$, u_τ being the wall friction velocity and ν the kinematic viscosity), turbulence production is particularly active and peaks around $y^+ \approx 12$ showing that non-homogeneity induced by production is not negligible, which is confirmed by $L_C/y < 1$ in that region. Furthermore, L_C is always below λ, which confirms that mean shear and turbulence production are significant at the very smallest scales of the inertial range and even below, i.e. at scales where viscosity matters. The non-linear turbulent transport is significant in the buffer region ($y^+ \le 30$) and becomes insignificant for $30 < y^+ \le 60$, which is reflected by the value of L_I/y which is below 1 at $y^+ \le 30$ and above 1 for $30 < y^+ \le 60$. Like L_C, L_I is also smaller than λ when non-linear turbulent transport is active, meaning that the very smallest scales r_x and r_z of the inertial range and even smaller scales where at where viscosity matters are affected by non-homogeneity induced by both mean shear and non-linear turbulent diffusion.

In the near-equilibrium region ($60 < y^+ \le Re_\tau/2$) where turbulent transport is negligible and dissipation is mainly balanced by production, L_I is always one to two orders of magnitude larger than the distance from the wall y. However, L_C is approximately proportional to y, which is a consequence of the approximate log-law of mean velocity profile, and it is smaller than y but larger than λ. This reflects the fact that statistical non-homogeneity is mainly introduced by mean shear and turbulent production in the near-equilibrium region and affects two-point statistics at scales larger than λ. The separation between L_C and λ increases with increasing wall distance and larger Reynolds number and leading to the emergence of an inertial range which is influenced by neither viscosity nor mean shear.

Entering into the core region ($y^+ > Re_\tau/2$), production decreases monotonically while a net transport rate of turbulent energy gradually increases from the near-equilibrium region and exceeds turbulence production where $y^+ > 0.8Re_\tau$. Accordingly, L_C steeply increases and tends to infinity as a consequence of $S \to 0$ as $y \to \delta$, meaning that non-homogeneity from mean shear and turbulence production does not influence two-point statistics in the central region ($y^+ > 0.9Re_\tau$). However, L_I decreases as $y/\delta \to 1$ and becomes even smaller than λ when $y^+ > 0.9Re_\tau$. Given that average turbulent energy fluxes converge from both walls towards the centreline, the flux at the centreline averages to zero and leads to $L_I \to 0$, which leads to the emergence of non-homogeneity at scales well below λ from turbulent fluctuations. The FD TCF's centreline region $y^+ > 0.9Re_\tau$, where there is minimal if any turbulence production and only non-linear turbulent transport acting as a source of energy, is therefore fertile ground for the study of the scale-by-scale behaviour of the non-linear terms in equation (2) for $\mathbf{r} = (r_x, 0, r_z)$.

Two-point statistics

Some examples of our results are plotted in figures 5 and 6. Firstly, the inter-scale and inter-space transfer rates are both negative and of comparable magnitude over all scales r_x (with $r_y = r_z = 0$) and over all scales r_z (with $r_x = r_y = 0$) sampled. Hence, scales equal to or smaller than r_x or r_z gain energy both from larger scales and from elsewhere in the flow. Indeed, non-linear turbulent diffusion is from the walls to the centreline, and this occurs at all scales. Secondly, the presence of non-vanishing inter-space transfer rates at scales as small or even smaller than the Taylor length λ means that the turbulence is locally non-homogeneous at such scales around the centreline. In agreement with our inter-space turbulence transfer results, $L_I < \lambda$ and $L_C \gg y$ shown in figure 4 clearly signals that local non-homogeneity due to turbulence transport is present down to scales smaller than λ in the core region where non-homogeneity due to turbulence production is absent at all scales.

We identify three length scale ranges in scale-by-scale transfer rate results such as those of figures 5 and 6. Firstly, at scales r_x (figure 5(a)) and r_z (figure 5(b)) larger than L_{0x} and L_{0z} respectively, Π, T_u and T_p converge towards their respective one-point transfer rates as expected. L_{0x} and L_{0z} are the lengths defined by the first zero-crossing of the respective fluctuating velocity two-point correlation functions.

Secondly, in the range of r_x between the integral length scale L_x and L_{0x} (figures 6(a) and 6(c)) and of r_z between integral scale L_z and L_{0z} (figure 6(b) and 6(d)), Π and T_u are constant with a $\log(r_x/y)$ correction. T_p is negative and constant (at about 11% of turbulence dissipation) without logarithmic correction for $L_x \leq r_x \leq L_{0x}$ whereas it is negative and constant with a $\log(r_z/y)$ correction for $L_z \leq r_z \leq L_{0z}$.

Thirdly, in the range $L_I < \lambda \leq r_x \leq L_x$, all three transfer rates, Π, T_u and T_p are constant with a $\log(r_x/y)$ correction (figure 6). Specifically,

$$-\Pi/\varepsilon \approx 0.62 - 0.054 \log(r_x/y),$$

$$-T_u/\varepsilon \approx 0.52 + 0.115 \log(r_x/y)$$

and

$$T_p/\varepsilon \approx -0.14 - 0.064 \log(r_x/y)$$

at $Re_\tau = 3000$. The same holds in the range $L_I < \lambda \leq r_z \leq L_z$ but with $T_p \approx 0$. Specifically,

$$-\Pi/\varepsilon \approx 0.41 - 0.15 \log(r_z/y)$$

and

$$-T_u/\varepsilon \approx 0.69 + 0.19 \log(r_z/y).$$

These results confirm the leading order predictions of the theory of non-homogeneous turbulent cascades in non-homogeneous turbulence without turbulence production recently developed by Chen & Vassilicos (2022) and Beaumard *et al.* (2024). Our results for the centreline region of FD TCF suggest logarithmic corrections to the constant leading orders and pave the way for investigations concerning higher orders, the range of validity of the hypothesis of homogeneous two-point physics in non-homogeneous turbulence, and what sets the actual dimensionless coefficients in equations such as the ones above.

CONCLUSION

Non-homogeneity causes a departure from Kolmogorov scale-by-scale equilibrium which manifests as different types of scale-by-scale non-equilibria in different types of non-homogeneity. By defining two non-homogeneity length scales one based on mean shear/turbulence production and the other on turbulent diffusion, different types of non-homogeneity are probed in different regions of a FD TCF: (i) in the near-wall region, the non-homogeneity is introduced by both mean shear/turbulence production and turbulent diffusion down to scales smaller than Taylor length; (ii) in near-equilibrium region, only the turbulence production contributes to the non-homogeneity outside viscous range of two-point separation lengths; (iii) in the central region, the turbulent diffusion is the main cause of non-homogeneity down to two-point separation lengths well below the Taylor length. In the near-equilibrium region, the non-homogeneity is driven by turbulence production and the scale-by-scale non-equilibrium can be explained in terms of the hypothesis of homogeneous two-point physics adapted to a turbulence production context as has been done by Apostolidis *et al.* (2023). This is a case where the presence of significant two-point turbulence production at all scales down to the Taylor length is vital for the scale-by-scale turbulent kinetic energy budget (Apostolidis *et al.*, 2023). In the FD TCF's centreline region where there is no turbulence production, non-homogeneity is driven by non-linear turbulent transport. The recently introduced length-scale L_I which captures scales of turbulent transport non-homogeneity but does not capture scales of mean flow non-homogeneity shows agreement with our finding that the inter-space turbulent energy transfer rate is not negligible all the way down to length scales below the Taylor length. At such scales, the FD TCF's core region is therefore locally non-homogeneous and scale-by-scale Kolmogorov equilibrium is absent and replaced by a new type of equilibrium described by the equations in the left column of this page.

The DNS data of FD TCF that we have used to estimate the two-point energy budget in the core region also show that both the inter-space and the inter-scale transfer rates are negative over all non-zero length scales sampled, signifying that turbulent kinetic energy is received at a given scale from larger scales and from neighbouring space. Inter-scale and inter-space turbulent kinetic energy transfer rates normalised by turbulence dissipation are constant with a logarithmic correction over an inertial range of length scales. The pressure-velocity rate of transfer is significantly smaller throughout the scales but present in all length-scale ranges except $\lambda \leq r_z \leq L_z$ where it vanishes.

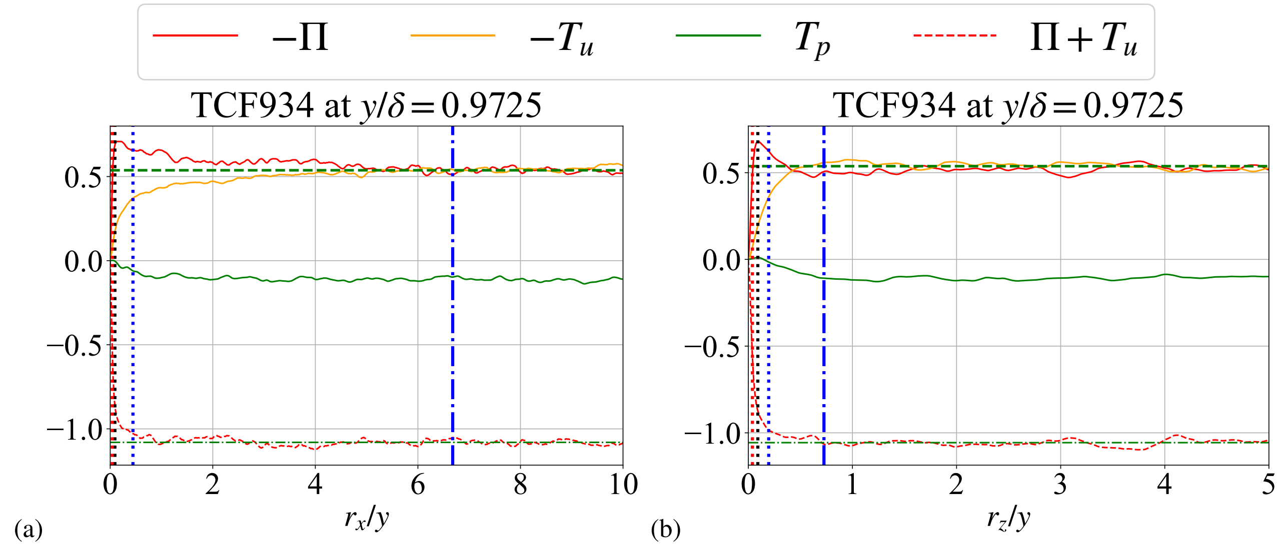

Figure 5. Non-linear inter-scale transfer rate Π, non-linear inter-space transfer rate T_u and pressure-velocity correlation term T_p at $y/\delta \simeq 1$ for TCF934, as functions of normalised streamwise (a) and spanwise separations (b). All terms are normalised by ε. The vertical lines from left to right indicate the non-homogeneity length L_I (red dotted line), the Taylor length (black dotted line), the integral length scale (blue dotted line), and the correlation zero-crossing length (blue dash-dotted line). The upper horizontal green dashed line corresponds to one-point turbulent transport of turbulent kinetic energy at the centroid. The lower horizontal green dash-dotted line corresponds to $\Pi + T_u \approx -1.08\varepsilon$ in (a) and $\Pi + T_u \approx -1.06\varepsilon$ in (b).

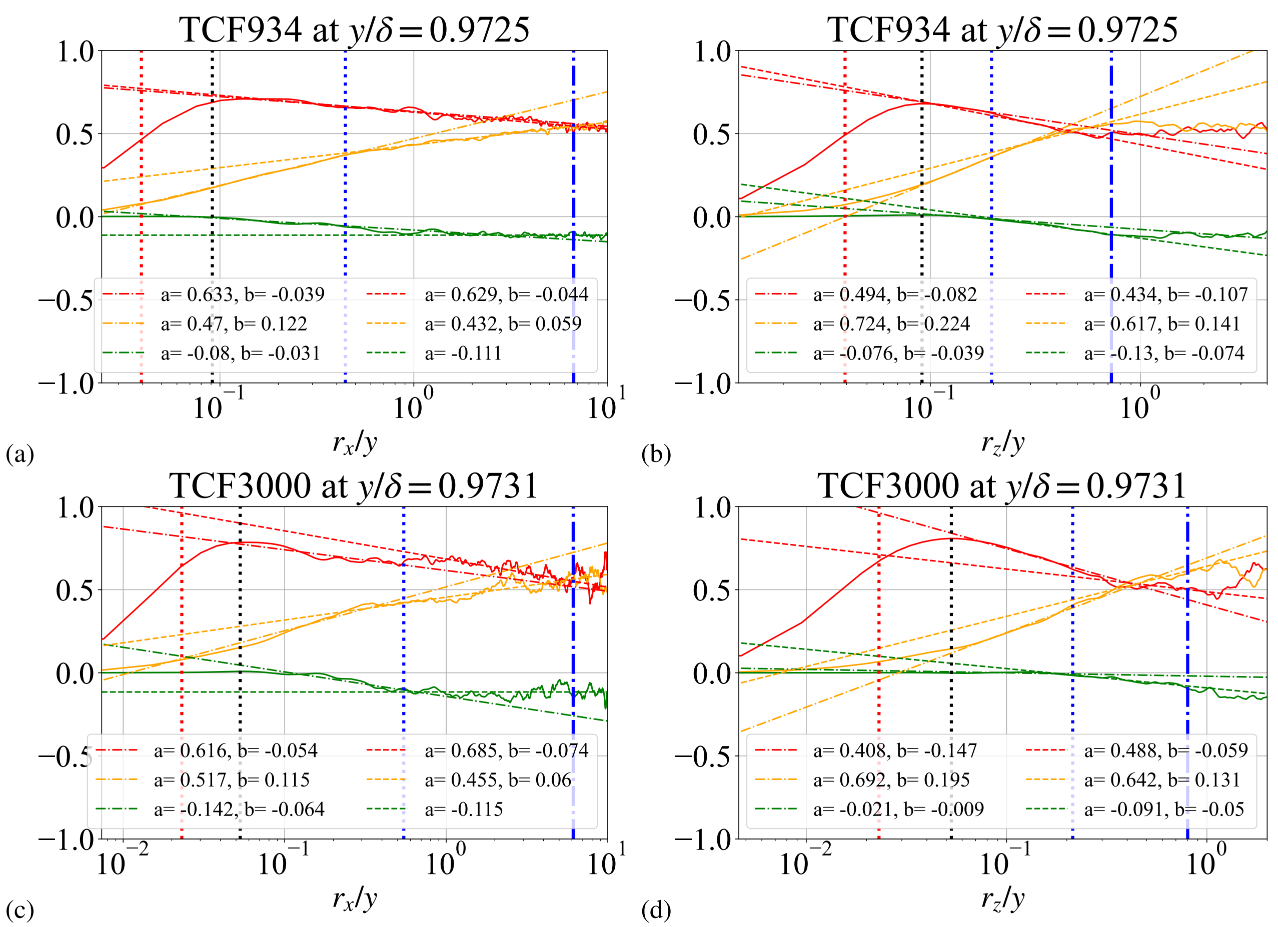

Figure 6. Log-law fits of Π, T_u and T_p at $y/\delta \simeq 1$ for TCF934 and TCF3000, as functions of normalised streamwise (a,c) and spanwise separations (b,d). The colours corresponding to different terms and vertical lines definitions are the same as in figure 5. The fitting lines are in the same colour as the terms they fit but with dash-dotted style for fitting in $\lambda < r_x < L_x$ & $\lambda < r_z < L_z$ and dashed style for fitting in $L_x < r_x < L_{0z}$ & $L_z < r_z < L_{0z}$. The coefficients shown in the legends are from the fitting function $a + b\log(r/y)$. Plots (a,b) for TCF934 and plots (c,d) for TCF3000.

ACKNOWLEDGEMENTS

This work was funded by the European Union (ERC, NoStaHo, 101054117). Views and opinions expressed are, however, those of the authors only and do not necessarily reflect those of the European Union or the European Research Council. Neither the European Union not the granting authority can be held responsible for them. This project was provided with computing HPC and storage resources by GENCI at IDRIS thanks to the grant 2025-A0182A01741 on the supercomputer Jean-Zay partition. We are grateful to Jean-Philippe Laval for his valuable assistance with and comments on this work.

REFERENCES

Apostolidis, A, Laval, JP & Vassilicos, JC 2023 Turbulent cascade in fully developed turbulent channel flow. *Journal of Fluid Mechanics* **967**, A22.

Beaumard, P, Bragança, P, Cuvier, C, Steiros, K & Vassilicos, JC 2024 Scale-by-scale non-equilibrium with kolmogorov-like scalings in non-homogeneous stationary turbulence. *Journal of Fluid Mechanics* **984**, A35.

Chen, JG & Vassilicos, JC 2022 Scalings of scale-by-scale turbulence energy in non-homogeneous turbulence. *Journal of Fluid Mechanics* **938**, A7.

Corrsin, S 1958 Local isotropy in turbulent shear flow. *Tech. Rep.*.

Dallas, V, Vassilicos, JC & Hewitt, GF 2009 Stagnation point von kármán coefficient. *Physical Review E—Statistical, Nonlinear, and Soft Matter Physics* **80** (4), 046306.

Frisch, U 1995 *Turbulence: The Legacy of A. N. Kolmogorov*. Cambridge University Press.

Hill, RJ 2002 Exact second-order structure-function relationships. *Journal of Fluid Mechanics* **468**, 317–326.

Hoyas, S & Jiménez, J 2008 Reynolds number effects on the reynolds-stress budgets in turbulent channels. *Physics of Fluids* **20** (10).

Noriega, EF & Vassilicos, JC 2026 Turbulent diffusion–cascade interaction. *Journal of Fluid Mechanics* **1028**, A3.

Thais, L, Tejada-Martı, AE, Gatski, TB, Mompean, G *et al.* 2011 A massively parallel hybrid scheme for direct numerical simulation of turbulent viscoelastic channel flow. *Computers & fluids* **43** (1), 134–142.

Valente, PC & Vassilicos, JC 2015 The energy cascade in grid-generated non-equilibrium decaying turbulence. *Physics of Fluids* **27** (4).